We are IntechOpen,
the world's leading publisher of
Open Access books
Built by scientists, for scientists

6,900
Open access books available

186,000
International authors and editors

200M
Downloads

154
Countries delivered to

Our authors are among the

TOP 1%
most cited scientists

12.2%
Contributors from top 500 universities

BOOK CITATION INDEX
CLARIVATE ANALYTICS
INDEXED

WEB OF SCIENCE™

Selection of our books indexed in the Book Citation Index
in Web of Science™ Core Collection (BKCI)

Interested in publishing with us?
Contact book.department@intechopen.com

Numbers displayed above are based on latest data collected.
For more information visit www.intechopen.com

Toward the Creation of Highly Active Photocatalysts That Convert Methane into Methanol

Yuichi Negishi, Seiichiro Watanabe, Marika Aoki, Sakiat Hossain and Wataru Kurashige

Abstract

Methane exists abundantly around Japan as methane hydrate. As the effective use of such methane, the conversion of methane into methanol has recently attracted much attention. Photocatalytic reaction is one of the methods which convert methane into methanol without using much energy. However, it is indispensable to improve the photocatalytic activity for their practical use. Our group has attempted to improve the activity of mesoporous tungsten trioxide and titanium dioxide (m-WO_3 and m-TiO_2) photocatalysts, which convert methane into methanol, by loading the ultrafine metal clusters as cocatalyst on the photocatalysts. As a result, we have succeeded in loading ultrafine metal-cluster cocatalysts onto m-WO_3 and m-TiO_2 and thereby improving their photocatalytic activity. Our study also demonstrated that the kind of metal element suitable for each photocatalyst depends on the kind of the photocatalysts, and thereby it is important to select the metal clusters suitable for each photocatalyst for improving its photocatalytic activity.

Keywords: photocatalyst, methane, methanol, activation, cocatalyst

1. Introduction

In recent years, the effective use of methane (CH_4) has attracted attention owing to the large amount of methane hydrate which is estimated to exist under the sea around Japan (**Figure 1(a)**) [1]. When CH_4 is burnt for generating energy, it generates small amounts of compounds which cause environmental problems, such as carbon dioxide, nitrogen oxide, and sulfur oxide (**Figure 1(b)**), [2]. Therefore, CH_4 can be used as a comparatively clean energy source. However, since CH_4 is a gas state at room temperature, it occupies a large volume and therefore costs for the transportation. On the other hand, if CH_4 is converted to liquid methanol (CH_3OH), the transportation costs could be reduced. Furthermore, the generated CH_3OH could be effectively used as a raw material for producing various chemical compounds. Therefore, in recent years, considerable attention has been focused on the development of a methodology for efficiently converting CH_4 into CH_3OH.

Regarding such a conversion, the current main methods require extreme conditions such as high temperature of around 500°C and high pressure of 50 atm or more [3]. Furthermore, since the reaction proceeds in two stages, the conversion consumes a large amount of energy. Therefore, many studies have been conducted to find a
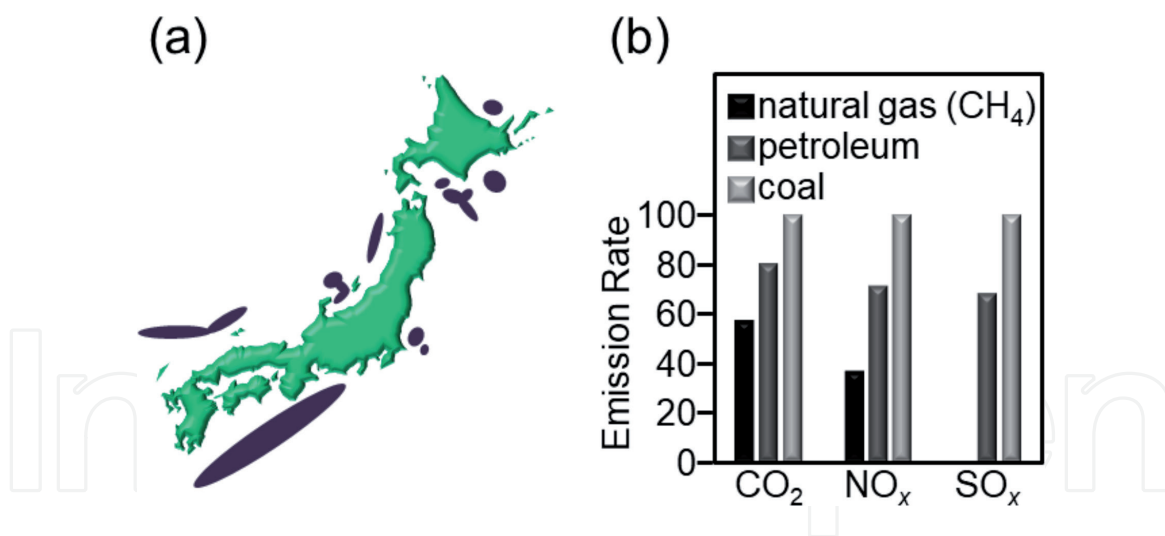
Figure 1.
(a) Estimated distribution of methane hydrate lying under the sea around Japan. (b) emission rate of each gas (CO_2, NO_x, or SO_x) from CH_4, petroleum, and coal. In (b), emission rate of each gas is normalized by letting the emission rate of CO_2 from coal be 100. Adapted from [1, 2].

method for the direct conversion of CH_4 to CH_3OH under mild conditions. However, most direct reactions require also high temperature and pressure conditions together with the use of an oxidizing agent [4]. Using a photocatalytic reaction for this conversion, the reaction can be conducted under moderate conditions [5]. However, the catalytic activity is still low, and further improvement is required for practical application. Then, our group has attempted to improve the photocatalytic activity of the photocatalyst used in this conversion. Our strategy was to load the controlled metal clusters on the surface of the photocatalyst as active sites (cocatalyst).

2. Research examples

Both tungsten oxide (WO_3) and titanium oxide (TiO_2) have redox potentials that are sufficient to generate hydroxyl radicals ($\cdot OH$) (**Figure 2(a)**), which is necessary for the reaction to proceed (**Figure 2(b)**) [6]. Furthermore, in their mesoporous structures (m-WO_3 and m-TiO_2), surface area becomes large and thereby the adsorption of reactive molecules is enhanced. In addition, in m-WO_3 and m-TiO_2, since the regular arrangement of pores suppresses the recombination of electrons and holes generated by the light irradiation, electrons and holes can be efficiently used in the reaction [7]. Then, in our study, we attempted to activate such m-WO_3 and m-TiO_2 by loading the ultrafine metal clusters as cocatalyst on the photocatalysts.

2.1 m-WO_3 photocatalyst

2.1.1 Preparation and loading of cocatalyst

m-WO_3 was prepared using a hard template method in the same manner as that reported in the literature [8]. First, mesoporous silica (KIT-6) was prepared to be used as a template (**Figure 3(a)**). Then, the obtained KIT-6 was mixed with 12-tungsto(VI) phosphoric acid n-hydrate ($H_3(PW_{12}O_{40})\cdot nH_2O$) in ethanol. The product was dried and then calcined at 350°C for 4 h. To the obtained powder, a further $H_3(PW_{12}O_{40})\cdot nH_2O$ ethanol solution was added and the mixture was stirred for 30 min. The product was again dried and then calcined at 550°C for 6 h. Finally, m-WO_3 was obtained by removing the KIT-6 template using hydrofluoric acid (HF) (**Figure 3(b)**).
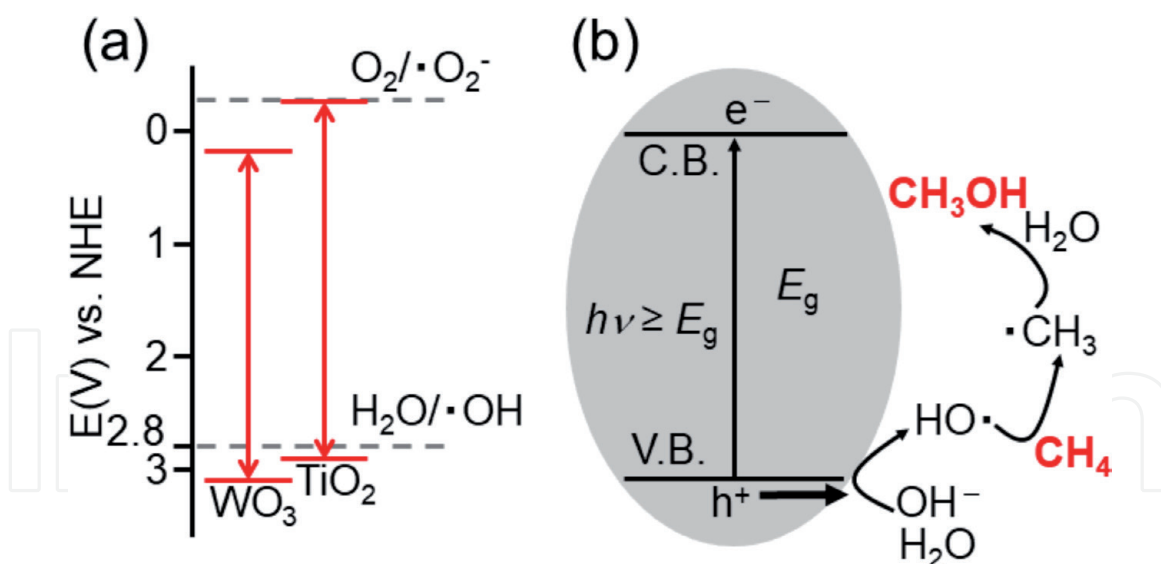
Figure 2.
(a) Redox potentials of WO_3 and TiO_2. Adapted from [4]. (b) Mechanism of the conversion of CH_4 to CH_3OH by photocatalytic reaction; C.B., V.B., and E_g indicate conduction band, valence band, and band gap, respectively.

Next, metal clusters were loaded onto the obtained m-WO_3. Our previous research on water-splitting photocatalysts [9–13] revealed that when a chemically-synthesized ligand-protected metal cluster is adsorbed onto a photocatalyst and its ligand is removed by the calcination, the controlled metal clusters can be loaded on the photocatalyst. Then, in this study, each metal cluster was loaded onto m-WO_3 using such a method (**Figure 3(c)**). Silver (Ag), nickel (Ni), and cobalt (Co) were chosen as metal element because they were expected to work as cocatalyst [14, 15]. Glutathionate (SG) was used as the ligand of the metal cluster. SG-protected silver clusters ($Ag_n(SG)_m$) were synthesized using the solid phase method reported by Bakr *et al* [16]. $Ni_n(SG)_m$ and $Co_n(SG)_m$ clusters were synthesized using the liquid phase method reported for SG-protected gold clusters ($Au_n(SG)_m$) [17]. The $M_n(SG)_m$ clusters (M = Ag, Ni, or Co) thus obtained were dissolved in water, and m-WO_3 was added to this solution to adsorb the $M_n(SG)_m$ clusters on m-WO_3 ($M_n(SG)_m$-m-WO_3; M = Ag, Ni, or Co). The obtained $M_n(SG)_m$-m-WO_3 was calcined at 500°C under atmospheric pressure to remove the ligand of the $M_n(SG)_m$ cluster, and thereby, each metal cluster was loaded on m-WO_3 (M_n-m-WO_3; M = Ag, Ni, or Co).

2.1.2 Structural characterization

In the transmission electron microscope (TEM) image of m-WO_3, pores of 10 nm or less were observed (**Figure 4(a,b)**). In the small angle X-ray diffraction (XRD) pattern of m-WO_3 (**Figure 4(c)**), similar to the literature [18], a peak assigned to the (211) plane of KIT-6 was observed, in addition to the peak attributed to the (110) plane derived from cubic $I4_132$ or $I4_332$. These results indicate that the synthesized m-WO_3 has an arranged structure with regular pores.

Figure 5(a,b) shows the TEM images of $Co_n(SG)_m$-m-WO_3 and Co_n-m-WO_3, respectively, as representative examples of photocatalysts after adsorption and calcination. Particles with a size of 0.93 ± 0.20 nm could be observed in the TEM image of $Co_n(SG)_m$-m-WO_3. This indicates that ultrafine $Co_n(SG)_m$ clusters were synthesized with a narrow distribution. Particles of a similar size (0.96 ± 0.19 nm) were also observed for Co_n-m-WO_3. This indicates that Co_n clusters were loaded onto m-WO_3 during calcination without the aggregation. Based on the bulk density of Co (8.900 g/cm^3), it can be estimated that each loaded particle contains about 40 Co atoms. The loading of ultrafine particles was similarly observed in other
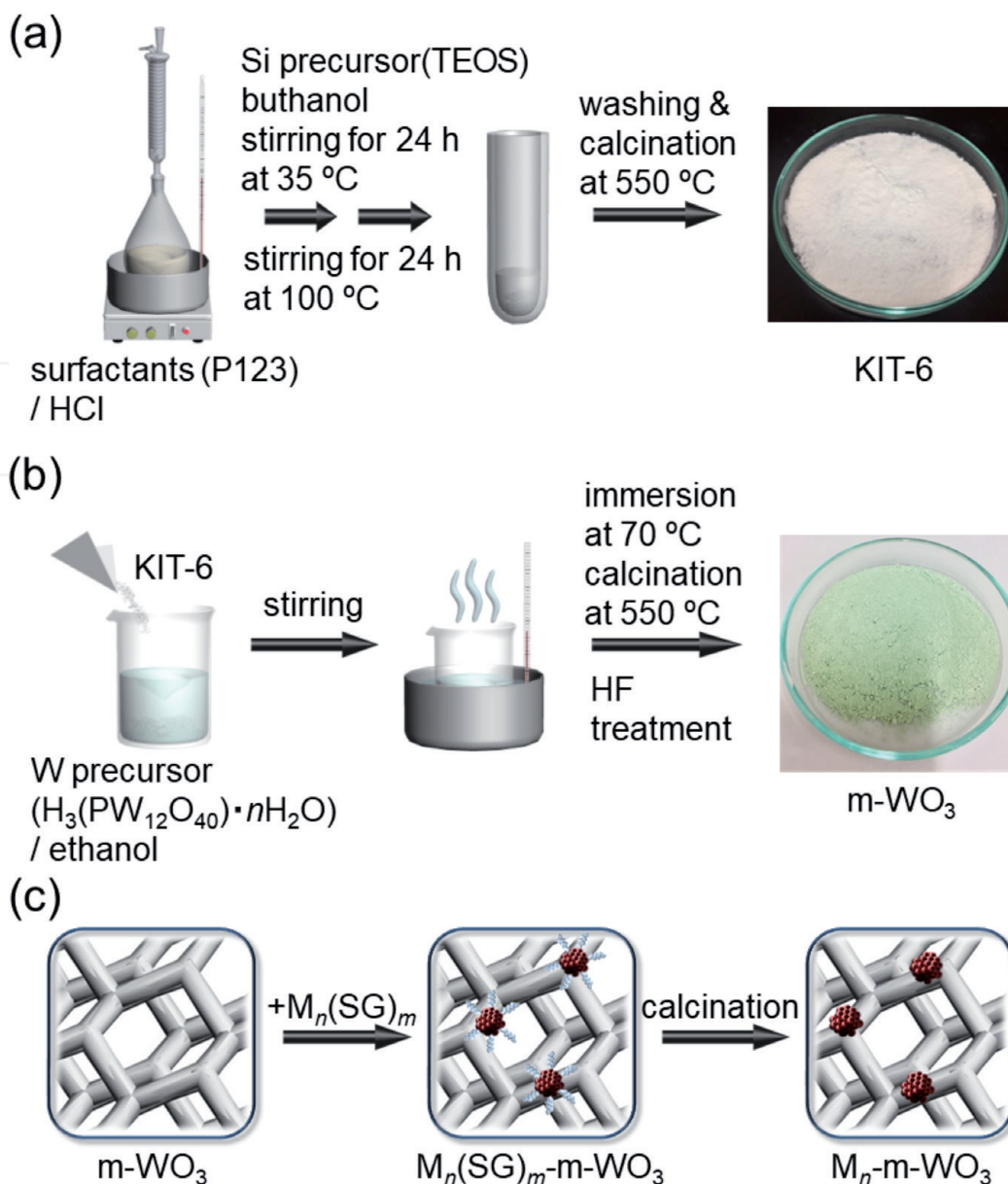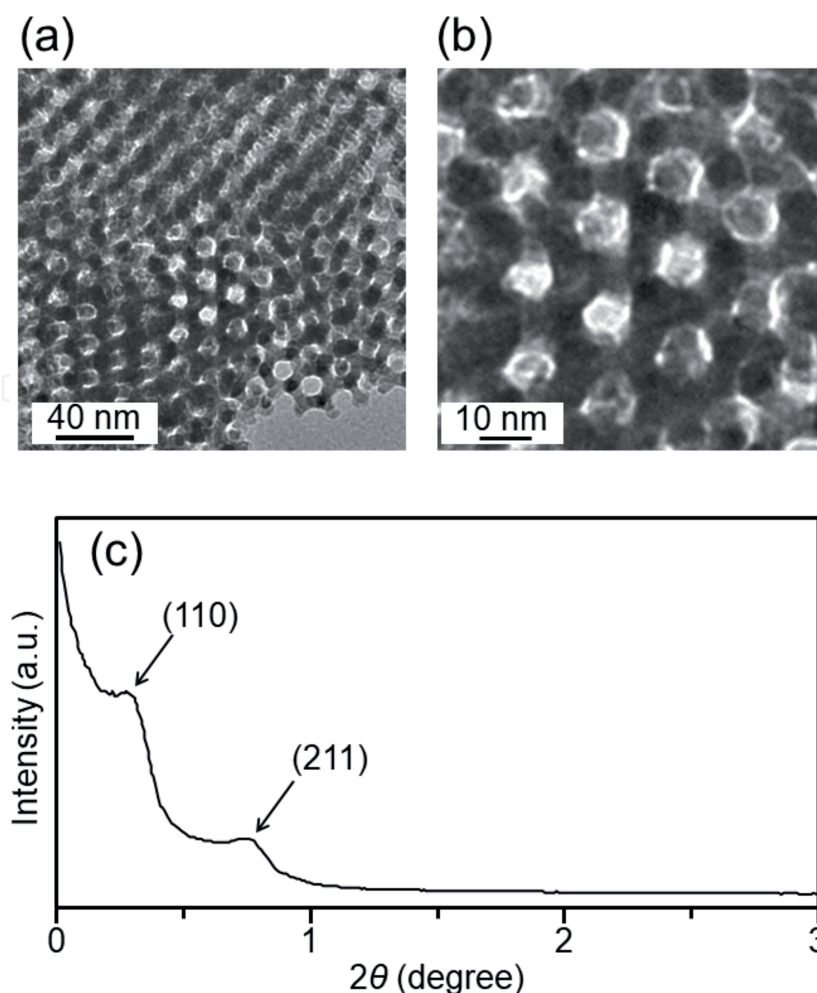
Figure 3.
Preparation methods of (a) KIT-6, (b) m-WO₃, and (c) Mₙ-m-WO₃ (M = Ag, Ni, or Co).

M_n-m-WO$_3$ (M = Ag or Ni). In this way, we have succeeded in loading ultrafine M_n clusters on m-WO$_3$ with a narrow size distribution.

2.1.3 Evaluation of photocatalytic activity

The photocatalytic activity was measured using an experimental apparatus built in-house consisting of a high-pressure mercury (Hg) lamp (400 W) and a quartz cell (**Figure 6**) [11]. First, 300 mg of M_n-m-WO$_3$ (M = Ag, Ni, and Co) was dispersed in 300 mL of water. Then, CH$_4$ and helium carrier gas were passed through this solution at a flow rate of 4.5–5 mL/min and 18 mL/min, respectively. The reaction was performed by the irradiation of ultraviolet light using a high-pressure Hg lamp. The temperature of the reaction system was maintained at 55–60°C by a circulator, and the gas generated by the reaction was analyzed with gas chromatography.

Figure 7 shows the rate of CH$_3$OH evolution from an aqueous solution containing M_n-m-WO$_3$ or m-WO$_3$. All the photocatalysts loaded with M_n clusters evolved CH$_3$OH at faster rate as compared with m-WO$_3$ without cocatalyst. This indicates

Figure 4.
*Characterization of m-WO₃. (a) TEM image, (b) expanded TEM image, and (c) small angle XRD pattern.*

that the loading of the M_n clusters improved the rate of the conversion of CH_4 to CH_3OH. It was found that the Co_n clusters have the largest improvement effect among the M_n clusters used in this study.

According to a previous study on m-WO₃ [8], in the conversion of CH_4 to CH_3OH, first, the holes generated via photoexcitation oxidize the hydroxyl groups (OH^-) on the photocatalyst surface and/or water (H_2O_{ad}) adsorbed on the surface to form ·OH radicals. The ·OH radicals have intense oxidizing power and attack CH_4 to generate methyl radicals (·CH_3). The ·CH_3 radicals thus produced react with H_2O to produce CH_3OH (**Figure 2(b)**). It can be considered that loading M_n clusters onto m-WO₃ promotes the charge separation between the electrons and holes, and thereby, the holes are efficiently consumed [15], leading to the improvement of the activity. It is presumed that highest activity was observed in the reaction using Co_n-m-WO₃, since the relationship between the positions of valence band of the photocatalyst and the orbitals of the loaded M_n cluster and/or the relationship between the redox potential of ·OH radical and that of the loaded M_n cluster was effective for accelerating the reaction in Co_n-m-WO₃ compared with the other photocatalysts (Ag_n-m-WO₃ or Ni_n-m-WO₃).
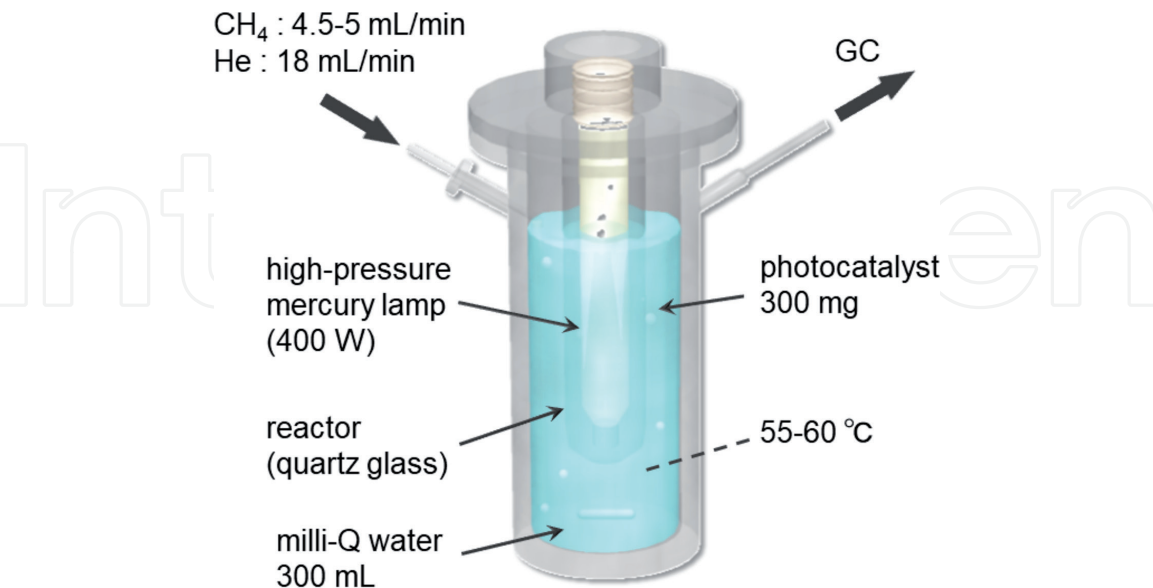
2.2 m-TiO₂ photocatalyst

2.2.1 Preparation and loading of cocatalyst

A m-TiO₂ photocatalyst was prepared according to a method reported in the literature [19]. Specifically, m-TiO₂ photocatalyst was prepared by forming a
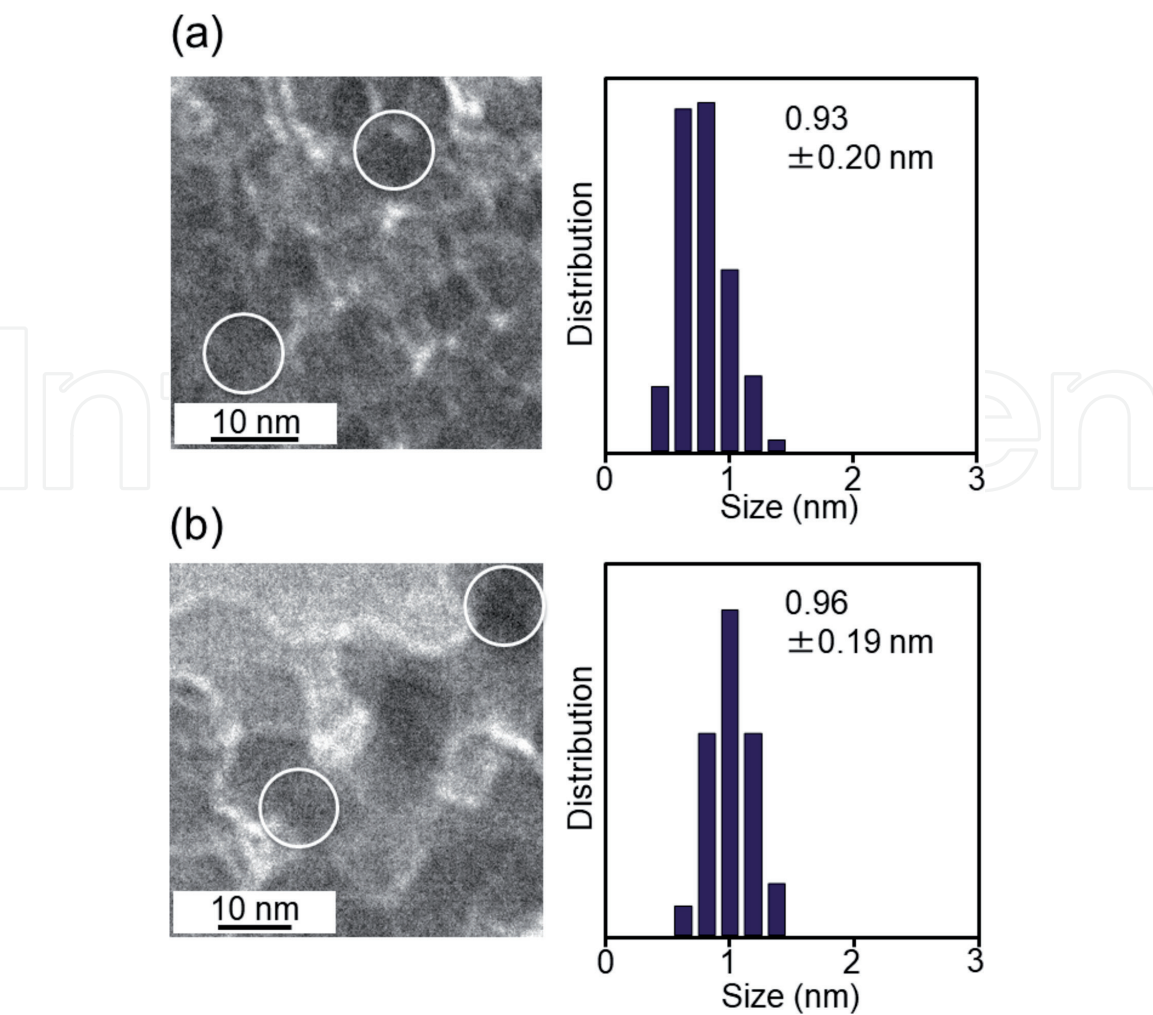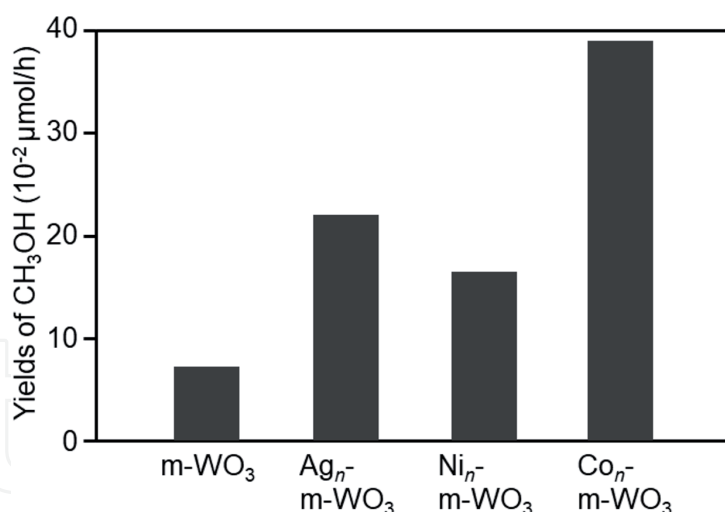
Figure 5.
TEM image and particle size distribution of (a) Co$_n$(SG)$_m$-m-WO$_3$ and (b) Co$_n$-m-WO$_3$. Multiple ultrafine particles can be seen in the white circles.
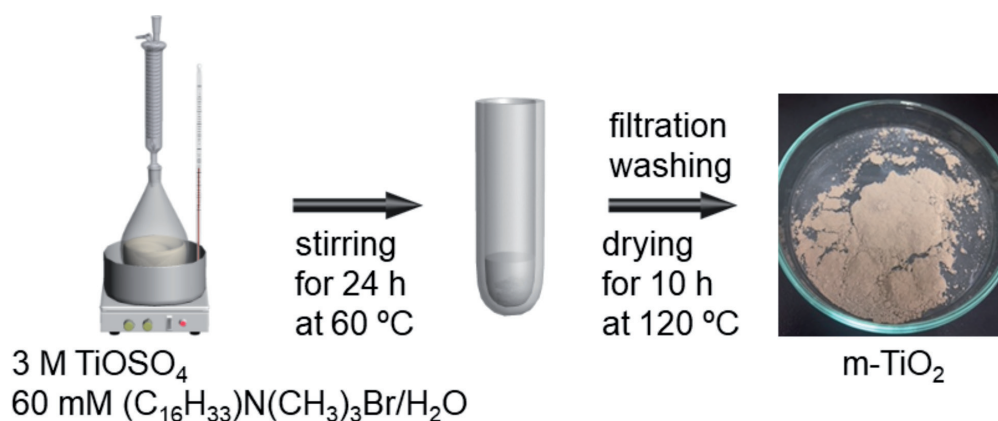

Figure 6.
Experimental apparatus built in-house consisting of a high-pressure mercury (Hg) lamp (400 W) and a quartz cell. GC means gas chromatograph.

photocatalyst around the micelle composed of surfactants. First, hexadecyltri-methylammonium bromide ($[(C_{16}H_{33})N(CH_3)_3]Br$) was added to an aqueous solution of titanyl oxysulfate sulfuric acid hydrate (TiOSO$_4$), and the solution

Figure 7.
Rate of CH₃OH evolution from an aqueous solution containing M_n-m-WO₃ or m-WO₃.

Figure 8.
Preparation methods of m-TiO₂.

was stirred at 60°C for 24 h. The obtained precipitate was washed with water and dried at 120°C for 10 h. Then, the dried sample was calcined at 450°C for 2 h to obtain m-TiO₂ (**Figure 8**). The M_n clusters (M = Ag, Ni, or Co) were loaded onto the surface of the obtained m-TiO₂ using the same method as that described for M_n-m-WO₃ (**Figure 3(c)**).

2.2.2 Structural characterization

Figure 9(a) shows a TEM image of the prepared m-TiO₂. It can be confirmed from this image that the material has a mesoporous structure different from that of m-WO₃ (**Figure 4(b)**). The diffuse reflection (DR) spectrum of m-TiO₂ revealed that the obtained m-TiO₂ has a band gap of around 3.24 eV, indicating that the obtained m-TiO₂ has an anatase type structure [19].

Figure 10(a) shows a TEM image of the $Ni_n(SG)_m$ cluster, as a representative example of a synthesized $M_n(SG)_m$ cluster. The particles with a size of 0.70 ± 0.14 nm can be observed in **Figure 10(a)**. On the other hand, the particles with a slightly larger size of 0.92 ± 0.17 nm were observed in the TEM image of Ni_n-m-TiO₂ (**Figure 10(b)**). This indicates that, in the synthesis of $Ni_n(SG)_m$-m-TiO₂, some cluster aggregation occurred during the adsorption or calcination processes. However, the size distribution of the observed particles is very narrow even for loaded particles. The number of Ni atoms contained in each particle was estimated to be about 40, based on the bulk density of Ni (8.908 g/cm³). Loading of such

ultrafine particles was similarly observed for the other M_n-m-TiO$_2$ (M = Ag or Co). These results indicate that m-TiO$_2$ ultrafine clusters were successfully loaded on a photocatalyst with a narrow distribution of the particle size.
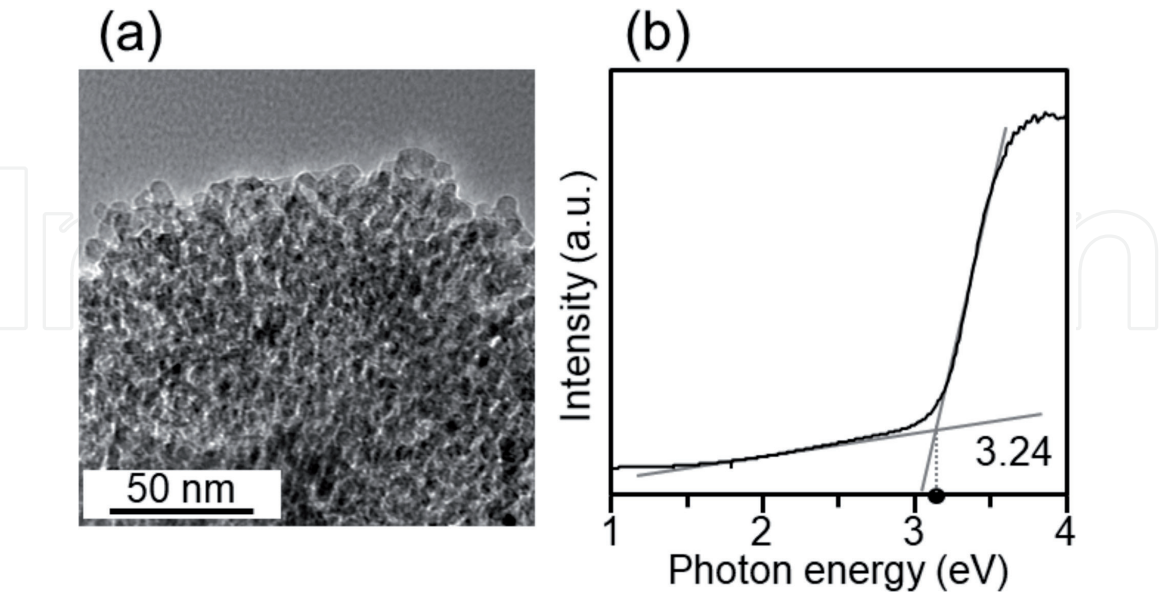
Figure 9.
Characterization of m-TiO$_2$. (a) TEM image and (b) DR spectrum.
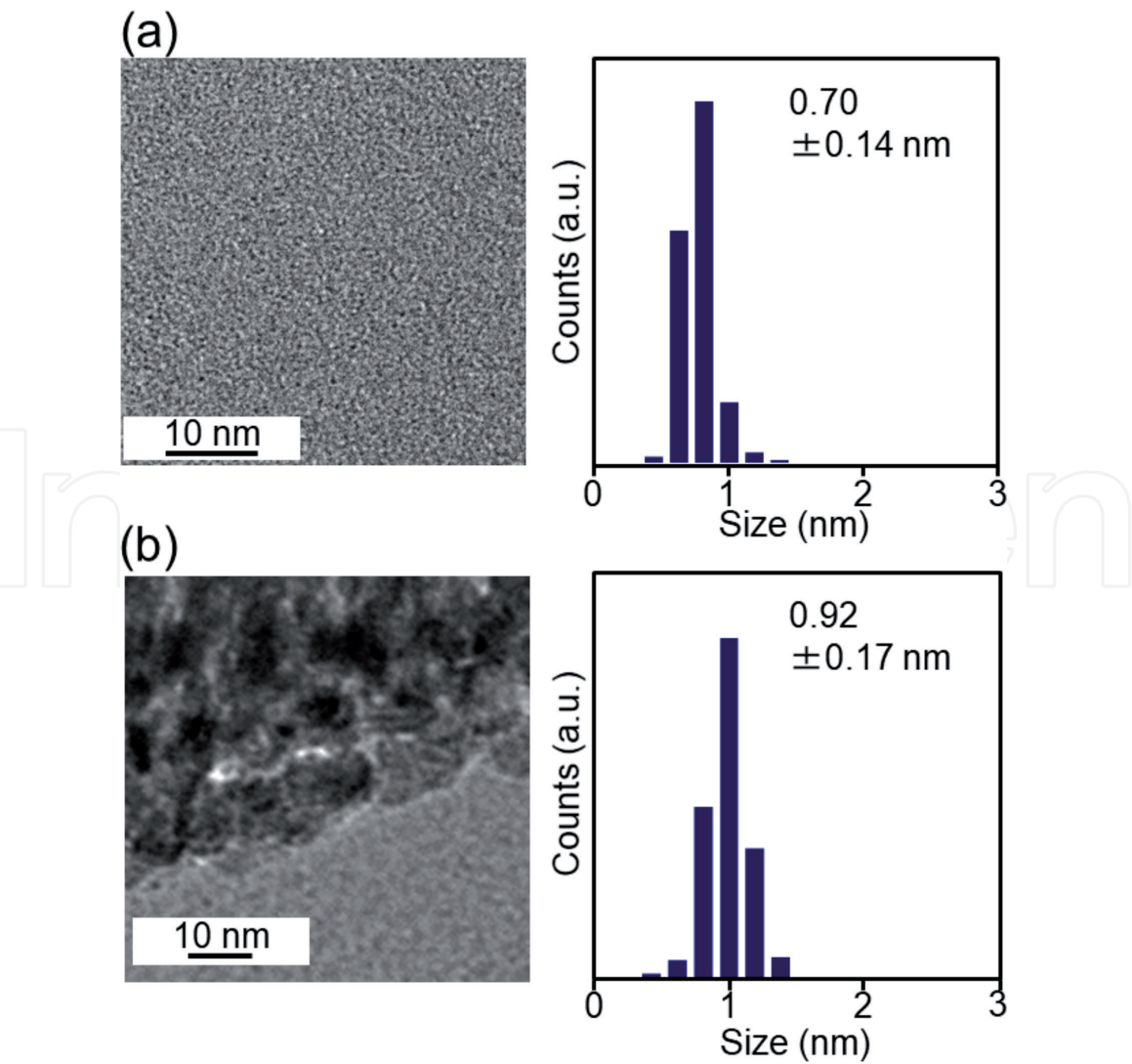
Figure 10.
TEM image and particle size distribution of (a) Ni$_n$(SG)$_m$ and (b) Ni$_n$-m-TiO$_2$.
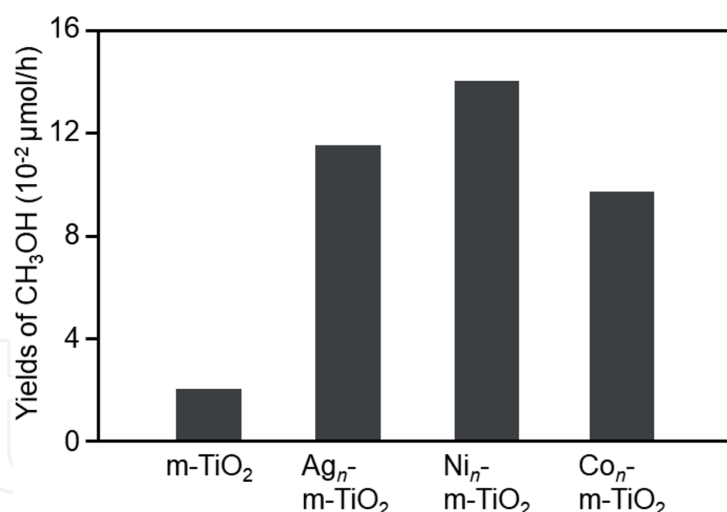
Figure 11.
Rate of CH_3OH evolution from an aqueous solution containing M_n-m-TiO_2 or m-TiO_2.

2.2.3 Evaluation of photocatalytic activity

The photocatalytic activity of a series of M_n-m-TiO_2 obtained in this manner was estimated in the same manner as that described in Section 2.1.3. **Figure 11** shows the rate of CH_3OH evolution from aqueous solutions containing either M_n-m-TiO_2 or m-TiO_2. Overall, the rate of CH_3OH evolution from M_n-m-TiO_2 or m-TiO_2 was lower than that from M_n-m-WO_3 or m-WO_3. Since the position of conduction band is relatively high in TiO_2 (**Figure 2(a)**), the superoxide radicals with strong oxidizing power can be generated from aqueous solution containing M_n-m-TiO_2 or m-TiO_2 by photoirradiation. It can be considered that since the superoxide radicals such generated attacked CH_3OH and thereby the excessive oxidation (decomposition) of CH_3OH occurred [20], the rate of the CH_3OH evolution decreased as a whole in the case of M_n-m-TiO_2 or m-TiO_2 compared to the case of M_n-m-WO_3 or m-WO_3. **Figure 11** also revealed that the loading of M_n clusters has the effect of promoting the conversion of CH_4 into CH_3OH also in the case of M_n-m-TiO_2.

On the other hand, regarding the metal elements, Ni showed a particularly high cocatalytic effect in M_n-m-TiO_2, unlike the case of m-WO_3 (**Figure 11**). The relationship between the position of the valence band of the photocatalyst and the position of the orbitals of the loaded M_n cluster and/or the relationship between the redox potential of ·OH radical and that of the loaded M_n cluster are considered to be strongly related to these phenomena. These results indicate that choosing an appropriate cocatalyst depending on the type of photocatalyst is very important to improve the photocatalytic activity.

3. Conclusions

Ultrafine M_n clusters (M = Ag, Ni, or Co) with a particle size of around 1 nm were successfully loaded onto m-WO_3 and m-TiO_2 with a narrow distribution. The photocatalytic activity measurements clearly demonstrated that the loading of such cocatalysts is effective in improving the activity for both types of photocatalysts. Furthermore, our study also revealed that it is important to appropriately selecting the element of the cocatalyst according to the photocatalyst to improve the photocatalytic activity. In these experiments, the particle diameter of the cocatalyst was reduced to approximately 1 nm to increase the reactive surface area. However, this size of a cocatalyst particle might not be optimal for promoting the reaction. In fact, our previous studies on water-splitting photocatalysts showed that extreme refining

of the cocatalyst particles reduces the activity per a surface atom of cocatalysts [8]. Therefore, in future studies, we would like to clarify the correlation between the particle size and activity of the cocatalyst. Furthermore, it seems also necessary to consider the method for efficiently consuming the excited electrons to accelerate the reaction.

Acknowledgements

Author details

Yuichi Negishi[1,2]*, Seiichiro Watanabe[1], Marika Aoki[1], Sakiat Hossain[1] and Wataru Kurashige[1]

1 Department of Applied Chemistry, Faculty of Science, Tokyo University of Science, Tokyo, Japan

2 Photocatalysis International Research Center, Tokyo University of Science, Chiba, Japan

*Address all correspondence to: negishi@rs.kagu.tus.ac.jp

IntechOpen

References

[1] Tsuji Y, Ishida H, Nakamizu M, Matsumoto R, Shimizu S. Overview of the MITI nankai trough wells: A milestone in the evaluation of methane hydrate resources. Resource Geology. 2004;**54**:3-10. DOI: 10.1111/j.1751-3928.2004.tb00182.x

[2] Pascoli SD, Femia A, Luzzati T. Natural gas, cars and the environment. A (relatively) 'clean' and cheap fuel looking for users. Ecological Economics. 2001;**38**:179-189. DOI: 10.1016/S0921-8009(01)00174-4

[3] Sushkevich VL, Palagin D, Ranocchiari M, Bokhoven JAV. Selective anaerobic oxidation of methane enables direct synthesis of methanol. Science. 2017;**356**:523-527. DOI: 10.1126/science.aam9035

[4] Zakaria Z, Kamarudin SK. Direct conversion technologies of methane to methanol: An overview. Renewable and Sustainable Energy Reviews. 2016;**65**: 250-261. DOI: 10.1016/j.rser.2016.05.082

[5] Zhu W, Shen M, Fan G, Yang A, Meyer JR, Ou Y, et al. Facet-dependent enhancement in the activity of bismuth vanadate microcrystals for the photocatalytic conversion of methane to methanol. ACS Applied Nano Materials. 2018;**1**:6683-6691. DOI: 10.1021/acsanm.8b01490

[6] Murcia-López SM, Villa K, Andreu T, Morante JR. Partial oxidation of methane to methanol using bismuth-Based photocatalysts. ACS Catalysis. 2014;**4**:3013-3019. DOI: 10.1021/cs500821r

[7] Li L, Krissanasaeranee M, Pattinson SW, Stefik M, Wiesner U, Steiner U, et al. Enhanced photocatalytic properties in well-ordered mesoporous WO_3. Chemical Communications. 2010;**46**:7620-7622. DOI: 10.1039/C0CC01237H

[8] Villa K, Murcia-López S, Andreu T, Morante JR. Mesoporous WO_3 photocatalyst for the partial oxidation of methane to methanol using electron scavengers. Applied Catalysis B: Environmental. 2015;**163**:150-155. DOI: 10.1016/j.apcatb.2014.07.055

[9] Negishi Y, Mizuno M, Hirayama M, Omatoi M, Takayama T, Iwase A, et al. Enhanced photocatalytic water splitting by $BaLa_4Ti_4O_{15}$ loaded with ~1 nm gold nanoclusters using glutathione-protected Au_{25} clusters. Nanoscale. 2013;**5**:7188-7192. DOI: 10.1039/c3nr01888A

[10] Negishi Y, Matsuura Y, Tomizawa R, Kurashige W, Niihori Y, Takayama T, et al. Controlled loading of small Au_n clusters (n = 10-39) onto $BaLa_4Ti_4O_{15}$ photocatalysts: Toward an understanding of size effect of cocatalyst on water-splitting photocatalytic activity. The Journal of Physical Chemistry C. 2015;**119**: 11224-11232. DOI: 10.1021/jp5122432

[11] Kurashige W, Kumazawa R, Ishii D, Hayashi R, Niihori Y, Hossain S, et al. Au_{25}-loaded $BaLa_4Ti_4O_{15}$ water-splitting photocatalyst with enhanced activity and durability produced using new chromium oxide shell formation method. The Journal of Physical Chemistry C. 2018;**122**:13669-13681. DOI: 10.1021/acs.jpcc.8b00151

[12] Negishi Y. Toward the creation of functionalized metal nanoclusters and highly active photocatalytic materials using thiolate-protected magic gold clusters. Bulletin of the Chemical Society of Japan. 2014;**87**:375-389. DOI: 10.1246/bcsj.20130288

[13] Kurashige W, Niihori Y, Sharma S, Negishi Y. Precise synthesis, functionalization and application of thiolate-protected gold clusters. Coordination Chemistry Reviews.

2016;**320-321**:238-250. DOI: 10.1016/j. ccr.2016.02.013

[14] Hameed A, Ismail IMI, Aslam M, Gondal MA. Photocatalytic conversion of methane into methanol: Performance of silver impregnated WO$_3$. Applied Catalysis A: General. 2014;**470**:327-335. DOI: 10.1016/j.apcata.2013.10.045

[15] Liu L, Ji Z, Zou W, Gu X, Deng Y, Gao F, et al. In situ loading transition metal oxide clusters on TiO$_2$ Nanosheets as Co-catalysts for exceptional high photoactivity. ACS Catalysis. 2013;**3**:2052-2061. DOI: 10.1021/cs4002755

[16] Bootharaju MS, Burlakov VM, Besong TMD, Joshi CP, AbdulHalim LG, Black DM, et al. Reversible size control of silver nanoclusters via ligand-Exchange. Chemistry of Materials. 2015;**27**:4289-4297. DOI: 10.1021/acs. chemmater.5b00650

[17] Negishi Y, Nobusada K, Tsukuda T. Glutathione-protected gold clusters revisited: bridging the gap between gold(I)−thiolate complexes and thiolate-protected gold nanocrystals. Journal of the American Chemical Society. 2005;**127**:5261-5270. DOI: 10.1021/ja042218h

[18] Rossinyol E, Arbiol J, Peiró F, Cornet A, Morante JR, Tian B, et al. Nanostructured metal oxides synthesized by hard template method for gas sensing applications. Sensors and Actuators B: Chemical. 2005;**109**:57-63. DOI: 10.1016/j.snb.2005.03.016

[19] Shibata H, Ogura T, Mukai T, Ohkubo T, Sakai H, Abe M. Direct synthesis of mesoporous titania particles having a crystalline wall. Journal of the American Chemical Society. 2005;**127**:16396-16397. DOI: 10.1021/ja0552601

[20] Gondal MA, Hameed A, Yamani ZH, Arfaj A. Photocatalytic transformation of methane into methanol under UV laser irradiation over WO$_3$, TiO$_2$ and NiO catalysts. Chemical Physics Letters. 2004;**392**: 372-377. DOI: 10.1016/j.cplett.2004.05.0